Check for updates

Chemistry–A European Journal

Research Article
doi.org/10.1002/chem.202203759

Chemistry Europe
European Chemical Societies Publishing

www.chemeurj.org

Surface Studies on the Energy Release of the MOST System 2-Carbethoxy-3-Phenyl-Norbornadiene/Quadricyclane (PENBD/PEQC) on Pt(111) and Ni(111)

Felix Hemauer,[a] Valentin Schwaab,[a] Eva Marie Freiberger,[a] Natalie J. Waleska,[a] Andreas Leng,[b] Cornelius Weiß,[b] Johann Steinhauer,[a] Fabian Düll,[a] Philipp Bachmann,[a] Andreas Hirsch,[b] Hans-Peter Steinrück,[a, c] and Christian Papp*[a, c, d]

Abstract: Novel energy-storage solutions are necessary for the transition from fossil to renewable energy sources. Auspicious candidates are so-called molecular solar thermal (MOST) systems. In our study, we investigate the surface chemistry of a derivatized norbornadiene/quadricyclane molecule pair. By using suitable push–pull substituents, a bathochromic shift of the absorption onset is achieved, allowing a greater overlap with the solar spectrum. Specifically, the adsorption and thermally induced reactions of 2-carbethoxy-3-phenyl-norbornadiene/quadricyclane are assessed on Pt(111) and Ni(111) as model catalyst surfaces by synchrotron radiation-based X-ray photoelectron spectroscopy (XPS). Comparison of the respective XP spectra enables the distinction of the energy-rich molecule from its energy-lean counterpart and allows qualitative information on the adsorption motifs to be derived. Monitoring the quantitative cycloreversion between 140 and 230 K spectroscopically demonstrates the release of the stored energy to be successfully triggered on Pt(111). Heating to above 300 K leads to fragmentation of the molecular framework. On Ni(111), no conversion of the energy-rich compound takes place. The individual decomposition pathways of the two isomers begin at 160 and 180 K, respectively. Pronounced desorption of almost the entire surface coverage only occurs for the energy-lean molecule on Ni(111) above 280 K; this suggests weakly bound species. The correlation between adsorption motif and desorption behavior is important for applications of MOST systems in heterogeneously catalyzed processes.

Introduction

The structural transition to renewable energy sources is one of the most decisive challenges of the 21st century. With a share of more than 76% of the primary energy consumption in Germany in 2021,[1] there is still a major dependence on fossil fuels. Moreover, the future of nuclear power generation is questionable due to safety concerns and political decisions.[2] Thus, green energy production is without alternative. However, in addition to geographical factors and seasonal fluctuations, there is no constant renewable power generation throughout a day. This intermittent character is especially pronounced for wind and solar energy. The resulting mismatch between load and demand of energy requires novel storing solutions.

One approach to tackle both energy production and energy storage are so-called molecular solar thermal (MOST) systems.[3] Unlike to photovoltaic devices, solar energy is captured and stored in a chemical manner. The energy-lean parent compound is converted to its energy-rich valence isomer by irradiation. In this process, a rearrangement of chemical bonds leads to strain within the molecular framework. Triggered thermally or catalytically, the back reaction releases the energetic difference on demand. The energy density strongly depends on the molecular weight and the reaction enthalpy of the photoconversion. Moreover, the absorption maximum of the energy-lean compound should coincide with the solar spectrum. Reversibility of the overall storage cycle and thermal stability also determine the feasibility of the considered systems.

[a] F. Hemauer, V. Schwaab, E. M. Freiberger, N. J. Waleska, Dr. J. Steinhauer, Dr. F. Düll, Dr. P. Bachmann, Prof. Dr. H.-P. Steinrück, Prof. Dr. C. Papp
Lehrstuhl für Physikalische Chemie II
Friedrich-Alexander-Universität Erlangen–Nürnberg
Egerlandstr. 3, 91058 Erlangen (Germany)
E-mail: christian.papp@fau.de

[b] A. Leng, Dr. C. Weiß, Prof. Dr. A. Hirsch
Lehrstuhl für Organische Chemie II
Friedrich-Alexander-Universität Erlangen–Nürnberg
Nikolaus-Fiebiger-Str. 10, 91058 Erlangen (Germany)

[c] Prof. Dr. H.-P. Steinrück, Prof. Dr. C. Papp
Erlangen Center for Interface Research and Catalysis (ECRC)
Friedrich-Alexander-Universität Erlangen-Nürnberg
Egerlandstr. 3, 91058 Erlangen (Germany)

[d] Prof. Dr. C. Papp
Physikalische und Theoretische Chemie
Freie Universität Berlin
Arnimallee 22, 14195 Berlin (Germany)

Supporting information for this article is available on the WWW under https://doi.org/10.1002/chem.202203759

© 2023 The Authors. Chemistry - A European Journal published by Wiley-VCH GmbH. This is an open access article under the terms of the Creative Commons Attribution License, which permits use, distribution and reproduction in any medium, provided the original work is properly cited.

© 2023 The Authors. Chemistry - A European Journal published by Wiley-VCH GmbH

Various compound classes have been suggested for MOST applications in literature. These include different azobenzenes,[4] stilbenes,[5] or fulvalene-tetracarbonyl-diruthenium[6] based systems. Herein, we investigate derivatives of the molecule pair norbornadiene (NBD) and quadricyclane (QC). The parent compounds are well known for several decades[7] and exhibit promising storage properties with a sufficient quantum yield for the photoconversion,[8] a reasonable long-term stability,[9] and a high reaction enthalpy of 89 kJ mol^{-1}.[10] However, the absorption onset of unsubstituted NBD at ~267 nm[11] has to be shifted to higher wavelengths for a better overlap with the solar spectrum.[12] Functionalization of the molecular framework leads to the desired bathochromic shift, but increases the molecular weight and, therefore, reduces the storage capacity. In addition, requirements concerning the thermal stability and facile isomerization into its energy-rich counterpart have still to be fulfilled. By now, numerous derivatives are available from synthesis.[11,13]

Insights into the surface chemistry at molecular scale during heterogeneously catalyzed processes provide crucial information for the path to real-life applications of the proposed model systems. Next to demonstrating successful isomerization and a triggered back reaction, stability boundaries and the interaction strength with the surface must be assessed. Our group investigated the cycloreversion reaction of unsubstituted QC to NBD and its thermal evolution on different catalyst surfaces. We found a high reactivity on Pt(111),[14] such that the conversion to NBD took place at temperatures below 125 K. On Ni(111),[15] the onset of the reaction of QC to NBD was determined to be ~168 K. The decomposition of NBD set in at about 190 K in both cases. In addition, first derivatives were studied on Ni(111). Results for 2,3-dibromonorbornadiene and its isomer[16] showed a partial dissociation of the bromine moieties at ~120 K. Nevertheless, the cycloreversion occurred at 170 K, while the subsequent reaction was equivalent to that found for the unsubstituted system. For 2,3-dicyano-norbornadiene and the corresponding isomer,[17] we observed intact adsorption at 130 K. The conversion reaction to the NBD derivative was monitored between 175 and 260 K, while thermal stability was given up to 290 K.

In this work, we discuss the adsorption and reaction behavior of 2-carbethoxy-3-phenyl-norbornadiene/quadricyclane (Figure 1), which is addressed in the following as phenyl-ester-NBD/QC (PENBD/PEQC), on Pt(111) and Ni(111). With its push-pull substituents, the absorption onset of this NBD derivate at 359 nm[18] is favorable, while the molecular mass is still reasonable with 240.3 g mol^{-1}. Synchrotron radiation-based X-ray photoelectron spectroscopy allows for in-situ measurements during adsorption. Temperature-programmed XPS (TPXPS) experiments were conducted to gain insights into the reaction pathway of both compounds on the two surfaces. In this way, we provide results on the feasibility of triggering the cycloreversion, and information about the thermal stability and decomposition. Thereby, another molecular design of norbornadiene/quadricyclane systems is evaluated.

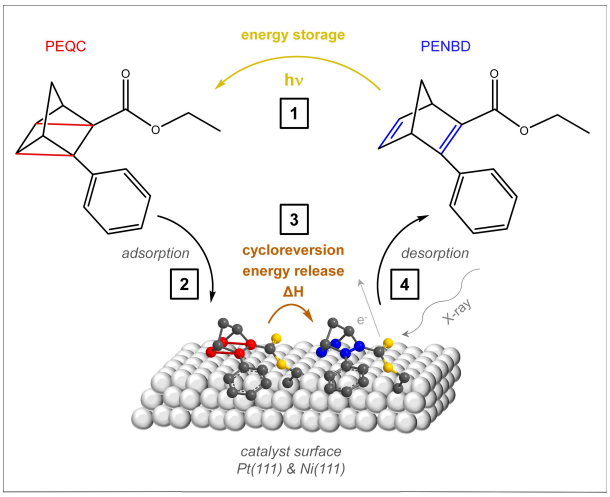

Figure 1. Scheme of the overall energy storage cycle of PENBD/PEQC as a proposed molecular solar thermal system: 1) Solar energy is captured and stored through irradiation of PENBD and isomerization to PEQC. 2) Adsorption of PEQC on a suitable catalyst material to trigger 3) the cycloreversion reaction back to PENBD under the release of energy on demand. 4) Desorption of the intact molecule for ideal total reversibility. XPS experiments conducted under UHV conditions are indicated by representation of the photoelectric effect.

Results and Discussion

The feasibility of the molecule pair 2-carbethoxy-3-phenyl-norbornadiene/quadricyclane (PENBD/PEQC) as a MOST system is addressed on different model catalyst surfaces, namely Pt(111) and Ni(111). In our study, we discuss in-situ HR-XPS measurements of the thermal evolution. In all experiments, the coverage was chosen to be in the sub-monolayer range to trace the reaction pathway without influence by possible physisorbed layers, which do not take part in the reaction. In the following, first C 1s spectra are evaluated, and the complementary O 1s region is described thereafter.

PENBD/PEQC on Pt(111): C 1 s region

We start with discussing the adsorption of PEQC and PENBD on Pt(111) at 125 K. Figure 2a depicts the evolution of the C 1s spectra with characteristic line shape upon exposing the clean surface (gray spectrum) to the energy-rich, strained PEQC. An exposure of 3.7 L resulted in a carbon coverage of 0.39 ML (red). The adsorption of the energy-lean counterpart PENBD is shown in Figure 2f; in this case, an exposure of 2.4 L at 125 K led to a coverage of 0.25 ML (blue). After the adsorption experiments, the temperature-programmed experiments were conducted by applying a constant heating rate ($\beta = 0.5$ K s^{-1}), while acquiring XP spectra continuously. Figure 2b depicts selected spectra of PEQC of the thermal evolution, and in Figure 2e the corresponding data of PENBD is shown. All XP spectra of the adsorption and TPXPS experiments are provided as density plots (Figure S2 in the Supporting Information). For a quantitative analysis of the adsorption and reaction behavior,

© 2023 The Authors. Chemistry - A European Journal published by Wiley-VCH GmbH

15213765, 2023, 25, Downloaded from https://chemistry-europe.onlinelibrary.wiley.com/doi/10.1002/chem.202203759 by Freie Universitaet Berlin, Wiley Online Library on [24/05/2023]. See the Terms and Conditions (https://onlinelibrary.wiley.com/terms-and-conditions) on Wiley Online Library for rules of use; OA articles are governed by the applicable Creative Commons License

Research Article
doi.org/10.1002/chem.202203759
Chemistry Europe
European Chemical Societies Publishing

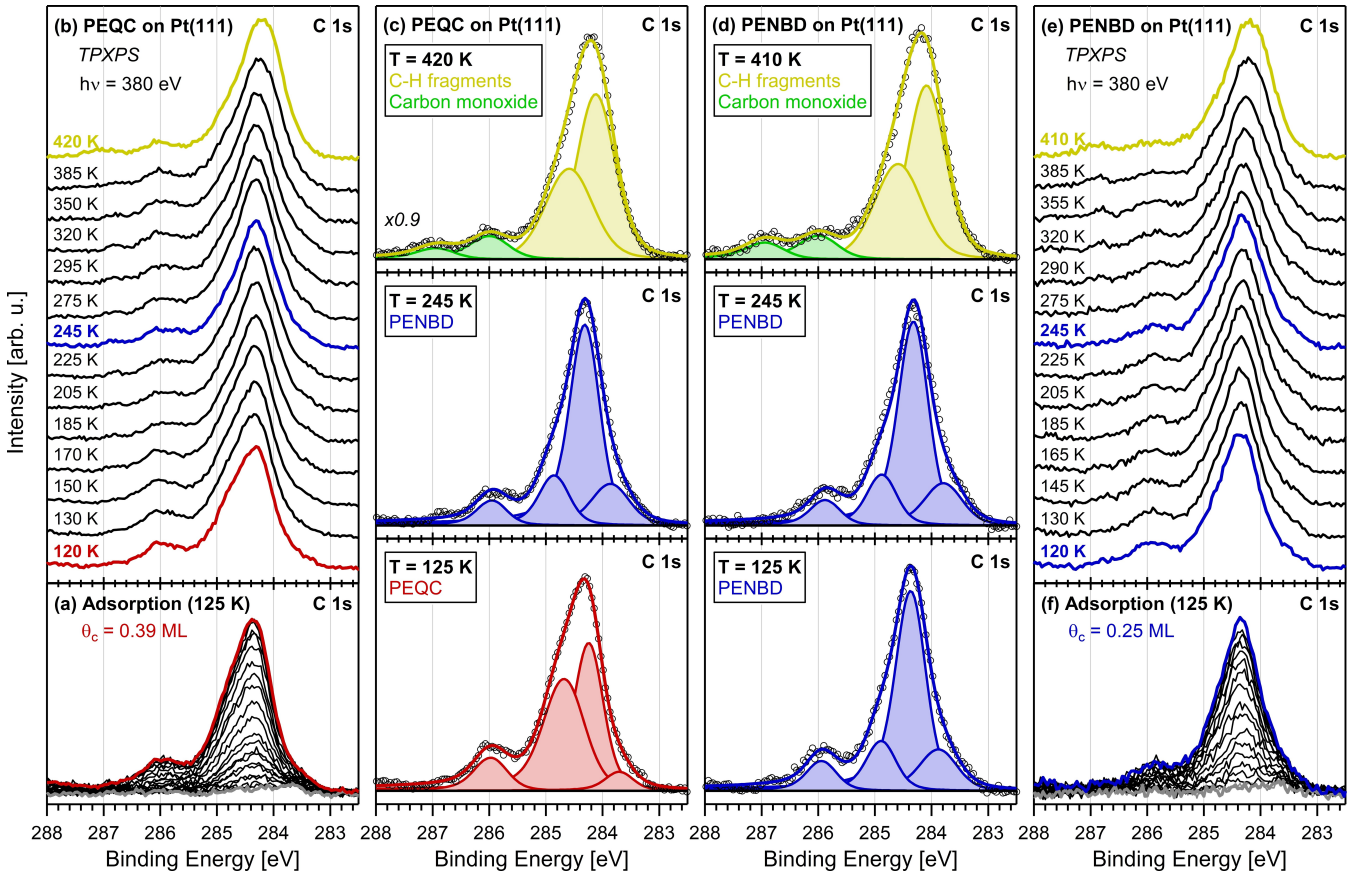

Figure 2. XP spectra of a) PEQC and f) PENBD in the C 1s region upon adsorption at low temperature on Pt(111); their characterisitc line shapes enable the molecules to be distinguished. The thermal evolution during temperature-programmed XPS (TPXPS) experiments is depicted for selected spectra of b) PEQC and e) PENBD as waterfall plots; c), d) spectra shown with fits are highlighted.

the data for both molecules have been fitted with a suitable fit model (see Table S1 for parameters).

We begin with the analysis of the data for adsorption of the energy-rich PEQC on Pt(111). Representative XP spectra along with their color-coded fits are shown in Figure 2c. At 125 K, the C 1s spectrum of PEQC (red) is fitted with four peaks at 283.7, 284.2, 284.7 and 286.0 eV with a fixed relative intensity ratio (1:8:8:2). Due to the large number of chemically very similar carbon atoms within the molecular structure and different possible orientations on the surface, the overlapping peaks cannot be assigned to individual carbon atoms in the molecules. The XP spectra rather serve as fingerprint of the investigated molecule. Nevertheless, we assume that the carbon atoms adjacent to the oxygen atoms of the ester moiety contribute to the peaks at higher binding energy.[19] The other peaks fall in the binding energy range known for unsubstituted quadricyclane on Pt(111) between 283.5 and 284 eV,[14] and benzene on Pt(111) between 284 to 285 eV.[20]

The result of peak fitting for the energy-lean PENBD is shown in Figure 2d for different representative temperatures. After adsorption of PENBD at 125 K (blue), at first sight, an overall similar line shape is detected as for PEQC. This is not surprising, as both molecular structures deviate by only two C–C bonds within the extended framework. However, closer inspection showed that quite different fit parameters have to be employed. Most notably is the difference of the relative intensity ratio (1:4:1:0.6) for PENBD, in comparison to PEQC (see above). While again four peaks describe the envelope of the measured spectra, the peaks are shifted to lower binding energies by 100 to 200 meV in comparison to PEQC, yielding values of 283.9, 284.4, 284.9 and 285.9 eV. In addition, the peak widths are different, that is, the peak at 283.9 eV is by 190 meV broader, whereas that at 284.9 eV is by 220 meV more narrow. As outlined above, a direct assignment of the respective signals to single atoms is not possible. Nevertheless, we again propose that the peak at highest binding energy correlates to the carbon atoms close to the ester group. Similar subtle differences in the spectral appearance have also been found for unsubstituted NBD/QC on Pt(111).[14] In summary, molecular adsorption of both PEQC and PENBD is observed, with each showing a distinct spectral fingerprint.

Next, we address the C 1s spectra during thermal evolution of PEQC on Pt(111). In Figure 2b, the waterfall plot shows selected spectra upon heating, and Figure 2c displays the peak fitting for the spectra at 125, 245 and 420 K. The corresponding quantitative analysis of all spectra of the heating series yields the coverage of the surface species in carbon MLs as a function of temperature in Figure 3; in addition, the proposed reaction

© 2023 The Authors. Chemistry - A European Journal published by Wiley-VCH GmbH

15213765, 2023, 25, Downloaded from https://chemistry-europe.onlinelibrary.wiley.com/doi/10.1002/chem.202203759 by Freie Universitaet Berlin, Wiley Online Library on [24/05/2023]. See the Terms and Conditions (https://onlinelibrary.wiley.com/terms-and-conditions) on Wiley Online Library for rules of use; OA articles are governed by the applicable Creative Commons License

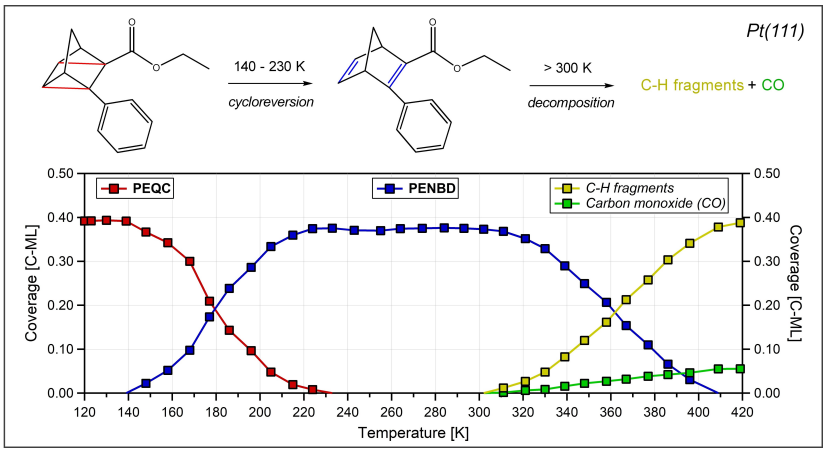

Figure 3. Quantitative analysis of the temperature-programmed XPS (TPXPS) experiment of PEQC in the C 1s region on Pt(111) coverage in carbon monolayers as a function of temperature: onset of the back reaction of PEQC to PENBD at 140 K, PENBD as solely surface species above 230 K, and decomposition into C–H fragements and CO when heating higher than 300 K; $\beta = 0.5\ \mathrm{K\,s^{-1}}$.

pathway of PEQC on Pt(111) is illustrated. The spectral appearance of PEQC stays unchanged until 140 K. Thereafter, the shoulder at ~285 eV loses intensity and the height of the maximum at ~284.4 eV increases. Overall, a transformation towards the line shape of PENBD at 125 K (Figure 2d, bottom) occurs. From the identical fit parameters at 245 K, we conclude that equivalent surface species exist. The onset of the cycloreversion reaction of PEQC to PENBD is at 140 K. Above this temperature, the surface coverage of PEQC is declining to the same extent as that of PENBD is increasing, while the total carbon amount remains constant. At 180 K, the amount of PENBD passes that of PEQC, and above 230 K, only PENBD is present on the surface (Figure 3). The unchanged total surface coverage and the absence of additional peaks indicate that no side reactions or desorption takes place and a quantitative conversion of PEQC to PENBD occurs. The observations for PEQC are in contrast to those for unsubstituted QC, which undergoes a direct back reaction to NBD upon adsorption on Pt(111) already at 125 K.[14] Therefore, steric and electronic influences by the push/pull-ligands and a different adsorption geometry hinder the catalytic activity on Pt(111) for the energy-rich PEQC derivative, so that a controlled conversion to energy-lean PENBD is observed at higher temperatures. Upon further heating, an analogous reaction behavior is found as for the PENBD experiment (see below).

The thermal evolution of PENBD can be analyzed from the TPXP spectra in Figure 2e and the selected fits in Figure 2d. Up to 300 K, no changes of the spectral line shape of PENBD are observed. Both the widths as well as the relative intensities remain constant; minor deviations of the peak positions by less than 100 meV towards lower binding energies are within the accuracy of measurement and evaluation. This observation indicates that the thermal stability of PENBD is relatively high, considering the fact that for unsubstituted NBD on Pt(111) already at 190 K the dissociation of a hydrogen atom from the bridgehead methyl group occurs.[14] This comparison suggest a different adsorption behavior of PENBD with no "side-on" geometry, implying that the bridgehead methyl group of the NBD unit does not point towards the surface. Above 300 K, a broadening of the main signal is found, which is fitted with two peaks at 284.1 and 284.6 eV (yellow). This indicates the onset of the decomposition of the molecular framework into unspecified C–H fragments as common dissociation products of hydrocarbons at elevated temperatures.[14,21] The two remaining peaks at higher binding energies, 286.0 and 286.9 eV (green) are ascribed to emerging carbon monoxide (CO), in accordance to literature values for bridge and on-top adsorption sites on Pt(111).[22] The amount of detected CO (Figure 3) matches the expected proportion of 12.5% (1/8) of the total fit area, implying the quantitative formation of two equivalents of CO for each decomposed molecule.

The complementary O 1s spectra of PEQC and PENBD on Pt(111) are given in Figure S1. However, due to coadsorption of water, the low oxygen content of the molecules and resulting rather low signal-to-noise ratio, less information can be derived. Moreover, the spectral differences of PEQC and PENBD are less pronounced in the O 1s spectra, since the structural differences only affect two pairs of carbon atoms within the NBD/QC framework, which are remote to the ester moiety. Thus, no distinction is possible in the O 1s region. Nonetheless, the stability boundaries are verified and the presence of carbon monoxide, in bridge and on-top position, is confirmed.

PENBD/PEQC on Ni(111): C 1s region

For comparison, we also addressed the adsorption and thermal evolution of PEQC and PENBD on Ni(111). The data is depicted and evaluated analogously to the Pt(111) experiments. The corresponding density plots of all measured XP spectra are given in Figure S3. Figure 4a shows the spectra during exposure of Ni(111) to the energy-rich, strained PEQC at 115 K leading to a characteristic line shape; the exposure of 1.4 L yielded 0.29 ML (red spectrum). Small intensities prior to the dosage (gray) are

© 2023 The Authors. Chemistry - A European Journal published by Wiley-VCH GmbH

15213765, 2023, 25, Downloaded from https://chemistry-europe.onlinelibrary.wiley.com/doi/10.1002/chem.202203759 by Freie Universitaet Berlin, Wiley Online Library on [24/05/2023]. See the Terms and Conditions (https://onlinelibrary.wiley.com/terms-and-conditions) on Wiley Online Library for rules of use; OA articles are governed by the applicable Creative Commons License

Research Article
doi.org/10.1002/chem.202203759
Chemistry Europe
European Chemical Societies Publishing

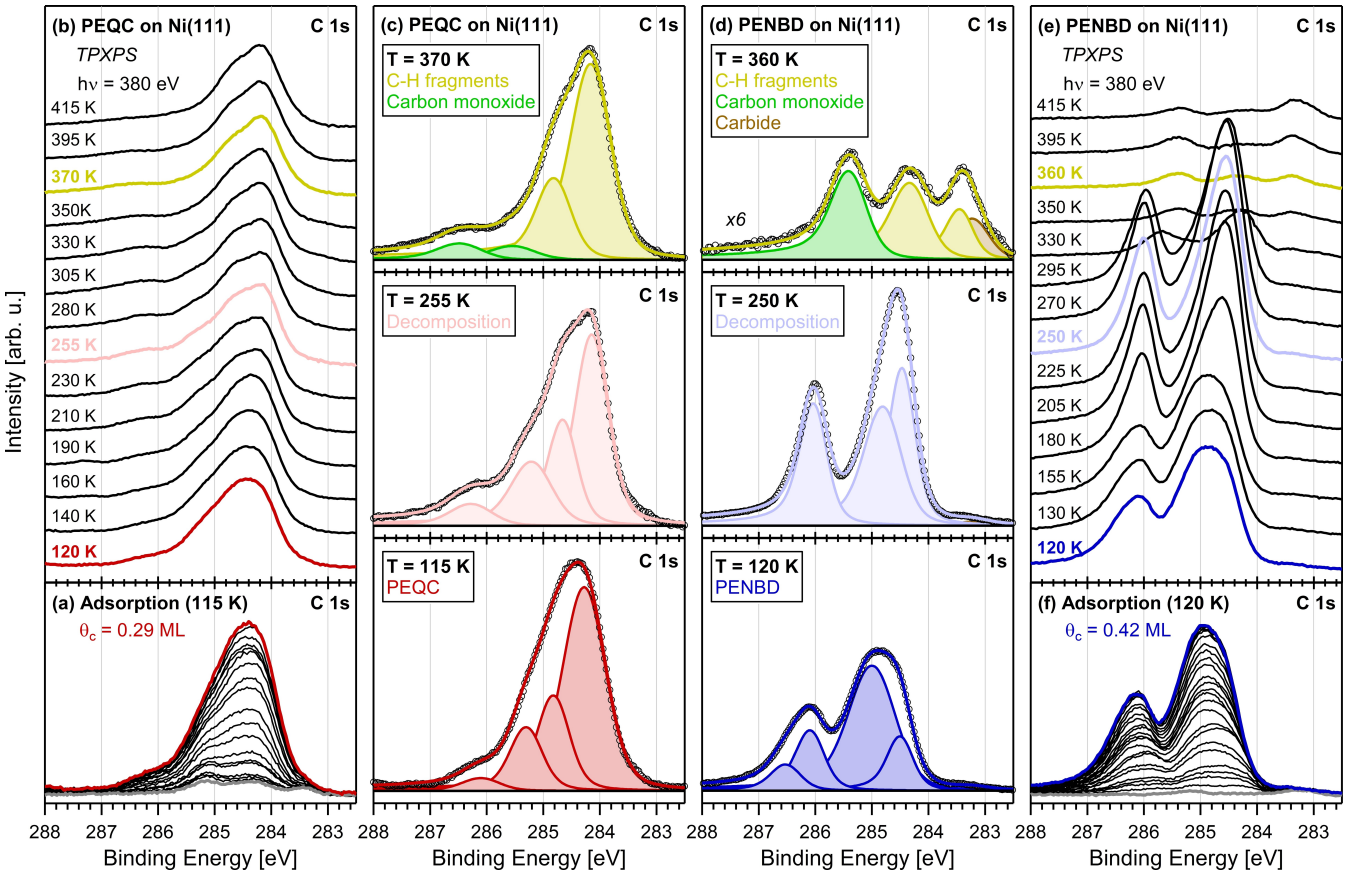

Figure 4. XP spectra of a) PEQC and f) PENBD in the C 1s region upon adsorption at low temperature on Ni(111); their characterisitc line shapes enable the molecules to be distinguished. The thermal evolution during temperature-programmed XPS (TPXPS) experiments is depicted for selected spectra of b) PEQC and e) PENBD as waterfall plots; c), d) spectra shown with fits are highlighted.

due to preadsorption of residual PEQC molecules in the chamber. The adsorption of the energy-lean PENBD at 120 K is depicted in Figure 4f (blue); here an exposure of 1.9 L resulted in a coverage of 0.42 ML. The subsequent TPXPS experiments of PEQC and PENBD are shown in Figure 4b and 4e, respectively. Again, the data was fitted for quantitative analysis (see Table S2 for parameters). Selected spectra of PEQC and PENBD along with their color-coded fits are shown in Figure 4c and d, respectively. The quantitative analyses of the thermal evolution are provided in Figure 5, wherein the coverages of the surface species are plotted against the temperature.

The spectrum after adsorption of PEQC on Ni(111) at 115 K (red) is fitted with four peaks at 284.3, 284.8, 285.3 and 286.1 eV with constant relative intensity ratio (10:3.7:2.5:0.7). As was the case for Pt(111), no direct assignment of the fitted peaks to single atoms within the molecular framework is possible, but the line shape serves as spectroscopic fingerprint of the investigated molecule. In literature, signals of unsubstituted QC on Ni(111) have been observed between 283.5 and 284.5 eV,[15] and those of benzene at slightly higher binding energies.[23] Thus, a convolution of these contributions plus those of the ester moiety up to 286.1 eV are in line with the observed spectrum of PEQC. Notably, while binding energy positions are comparable to the values of PEQC on Pt(111) (see above), their relative intensities are different and the FWHM is higher on Ni(111).

After adsorption of PENBD on Ni(111) at 120 K, the C 1s spectrum in Figure 4d (blue) displays a very different line shape from that of PEQC, with two separated strong signals. Fitting yields four peaks at 284.5, 285.0, 286.1 and 286.5 eV, with fixed relative intensity ratio (1:3.7:1.2:0.5); the peaks are individually shifted by up to 800 meV towards higher binding energies and show other widths compared to PEQC/Ni(111). The minor contribution at 283.2 eV (1.2% of total intensity) is assigned to carbide,[24] which is present on the surface prior to the adsorption and does not change during the experiment. Again, no attribution to single atoms is possible from the fitted peaks. Since there are only slight structural differences between PEQC and PENBD, it is surprising to find such strongly differing spectral shapes after adsorption on Ni(111), unlike to the situation on Pt(111). Next to different electronic influences of the substrate, an additional cause for this behavior is the possible coexistence of different adsorption geometries of PEQC and PENBD, which will be discussed later in the O 1s section.

The thermal evolution of PEQC on Ni(111) is shown in the waterfall plot in Figure 4b, along with selected fits in Figure 4c; the quantitative analysis of all data is given in Figure 5a. Line

© 2023 The Authors. Chemistry - A European Journal published by Wiley-VCH GmbH

15213765, 2023, 25, Downloaded from https://chemistry-europe.onlinelibrary.wiley.com/doi/10.1002/chem.202203759 by Freie Universitaet Berlin, Wiley Online Library on [24/05/2023]. See the Terms and Conditions (https://onlinelibrary.wiley.com/terms-and-conditions) on Wiley Online Library for rules of use; OA articles are governed by the applicable Creative Commons License

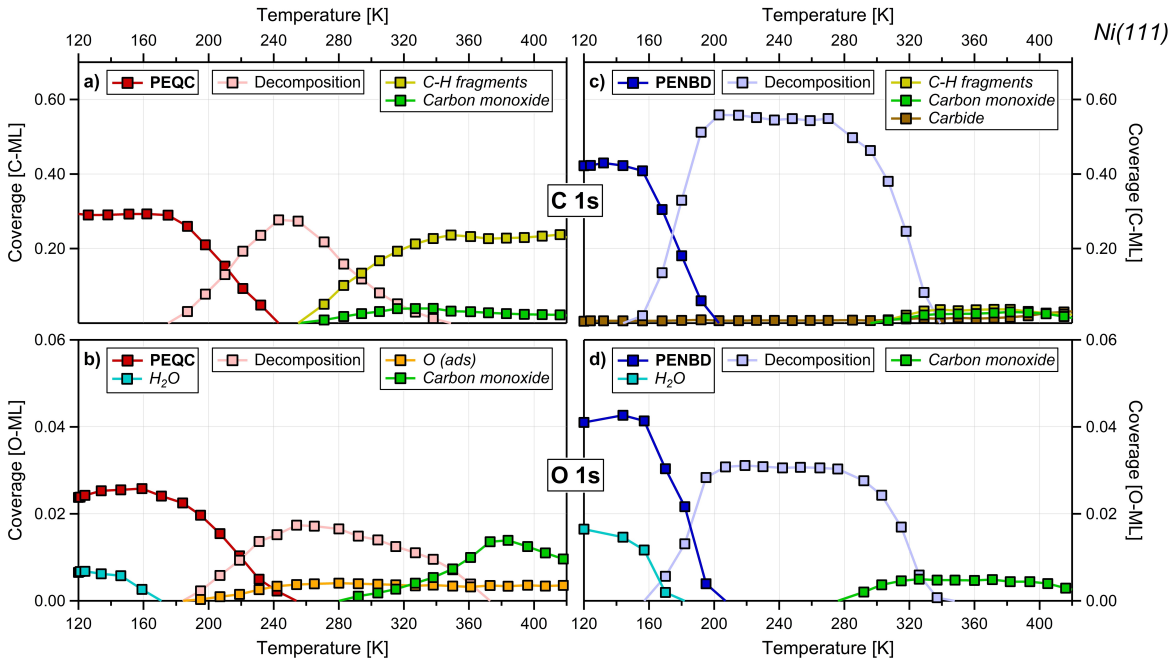

Figure 5. Quantitative analysis of the TPXPS experiments on Ni(111) of a) PEQC in the C 1s region, b) PEQC in the O 1s region, c) PENBD in the C 1s region, and d) PENBD in the O 1s region. Respective surface species are color coded, and their coverages are given in corresponding monolayers as a function of temperature; $\beta = 0.5\ \mathrm{K\,s^{-1}}$.

shape and coverage remain unchanged, until above 180 K small changes in the spectral appearance and an overall shift to lower binding energies are observed, indicating a transformation of the surface species that is complete at ~240 K; four new peaks at 284.1, 284.6, 285.2 and 286.3 eV are employed in order to obtain a satisfying fit (Figure 4c, light red). Three are shifted to lower binding energies by up to 200 meV, and only the peak at 286.3 eV shifts to higher binding energies by 200 meV. In addition, the relative intensity ratios change, in particular yielding a lower intensity for the peak with the lowest binding energy due to a more narrow line shape. Therefore, a rearrangement of the molecule on the surface, similar to what has been reported for dicyanonorbornadiene,[17] and/or decomposition reactions[25] are proposed. Compared to PENBD at equivalent temperatures, the line shape differs significantly. This is true for every spectrum during the thermal evolution of the molecular pair indicating no cycloreversion of PEQC to PENBD or even the presence of identical surface species at any temperature on Ni(111). Instead, individual decomposition routes are found. The stability boundaries are similar to unsubstituted and dibromo-substituted NBD/QC on nickel.[15–16]

Upon further heating PEQC to above 270 K, another characteristic change of the line shape is seen. The spectra are fitted by four new peaks at 284.1, 284.8, 285.5 and 286.4 eV (Figure 4c), with no change in total coverage (Figure 5a) and thus no desorption, which is in contrast to the behavior of PENBD (see below). The peaks at 285.5 and 286.4 eV (green) are ascribed to CO on bridge site and on top site, respectively; small shifts to higher binding energies compared to clean Ni(111) are attributed to coadsorption of hydrogen and oxygen.[26] As for PEQC/Pt(111), two equivalents of CO are formed for each decomposed PEQC molecule, since the fit area of CO (~12%; Figure 5a) agrees with the stoichiometric ratio of 1/8. The two remaining peaks at 284.1 and 284.8 eV are due to residual unspecified C–H fragments on the surface (yellow).[27]

The thermal evolution of PENBD on Ni(111) is shown in the waterfall plot in Figure 4e and selected fits in Figure 4d. The line shape and coverage (Figure 5c) remains unchanged up to 160 K. Thereafter, the spectroscopic appearance shows a pronounced change, and the C 1s spectra are now fitted with three new peaks at 284.5, 284.8 and 286 eV (Figure 4d, light blue). Thus, this temperature marks the onset of the first reaction step. Simultaneously, we find a significant change in the O 1s region (see below). These observations indicate a decomposition of the molecular framework, likely with a detachment of the ester moiety.[28] In contrast to unsubstituted NBD and dibromo-substituted NBD on Ni(111),[15–16] there are no indications for the formation of methylidyne or benzene.[23,29] Interestingly, the total carbon amount rises by 30% to 0.56 ML at 205 K, when the signals of intact PENBD have vanished. Since no additional carbon was supplied to the surface, we attribute this observation to a lower attenuation of the photoelectrons due to the reaction step and/or different photoelectron diffraction conditions for the distributed fragments in comparison to the bulky molecule (note the high surface sensitivity and multiple scattering effects at the chosen low kinetic energy of the photoelectrons of ~100 eV).[30] Starting at 280 K, a pronounced decrease of the total coverage to a residual coverage of 0.06 ML at 340 K is observed in Figure 5c (that is, a decline of more than 87%), indicative of nearly complete

© 2023 The Authors. Chemistry - A European Journal published by Wiley-VCH GmbH

15213765, 2023, 25, Downloaded from https://chemistry-europe.onlinelibrary.wiley.com/doi/10.1002/chem.202203759 by Freie Universitaet Berlin, Wiley Online Library on [24/05/2023]. See the Terms and Conditions (https://onlinelibrary.wiley.com/terms-and-conditions) on Wiley Online Library for rules of use; OA articles are governed by the applicable Creative Commons License

desorption of all surface species. This strong desorption is rather uncommon for extended hydrocarbon molecules. We explain this behavior by a weak interaction of the decomposition fragments with the nickel surface. With support of the O 1s data (see below), a less stable adsorption motif of PENBD is proposed. Next to the present carbide at 283.2 eV, the remaining signal above 340 K is fitted with three peaks at 283.4, 284.3 and 285.4 eV (Figure 4d). While the latter peak (green) is assigned to CO in bridge position,[26] the other two peaks (yellow) are attributed to C–H fragments.[27]

PENBD/PEQC on Ni(111): O 1 s region

Complementary information on adsorption and reaction of PEQC and PENBD on Ni(111) is obtained from TPXPS in the O 1s region. All XP spectra are depicted as density plots in Figure S3. The spectra collected during adsorption of the energy-rich PEQC at 120 K are shown in Figure 6a; an exposure of 1.1 L yielded a final coverage of 0.19 carbon ML (red spectrum). Prior to the adsorption (gray), contributions due to preadsorption from residual PEQC in the chamber are visible. The spectra during adsorption of the energy-lean PENBD are shown in Figure 6f; here, an exposure of 1.5 L yielded 0.32 carbon ML (blue). The subsequent TPXPS measurements are depicted as waterfall plots in Figure 6b for PEQC and Figure 6e for PENBD. Analogous to the C 1s experiment, the spectra are fitted for quantitative analysis (see Table S2 for parameters).

Figure 6c depicts the O 1s spectra of PEQC on Ni(111) at selected temperatures along with their color-coded fits. The quantification of the data is given in Figure 5b. After adsorption at 120 K (red), two distinct signals are observed. For the fit model, three peaks at 531.7, 533.1 and 533.3 eV are employed to reproduce the line shape. Since the total carbon coverage stays constant up to ~250 K (Figure 5a) but the total oxygen O 1s coverage decreases by almost 30%, we conclude that coadsorbed water contributes to the O 1s signal. We attribute the peak at 533.1 eV in Figure 6c (turquoise) to water, as its binding energy and desorption temperature match literature values on Ni(111).[31] The two peaks at 531.7 and 533.3 eV (red) are assigned to PEQC, as expected for two inequivalent oxygen atoms in the molecule; accordingly, the areas of both peaks are identical. The peak at 533.3 eV stems from the ether oxygen (C–O–C) within the ester moiety, and the peak at 531.7 eV from the carbonyl oxygen (C=O). Notably, the latter one exhibits a narrower peak width by 625 meV, which is explained by the more constrained flexibility of the double bound oxygen atom. The binding energy difference of 1.6 eV of both oxygen atoms

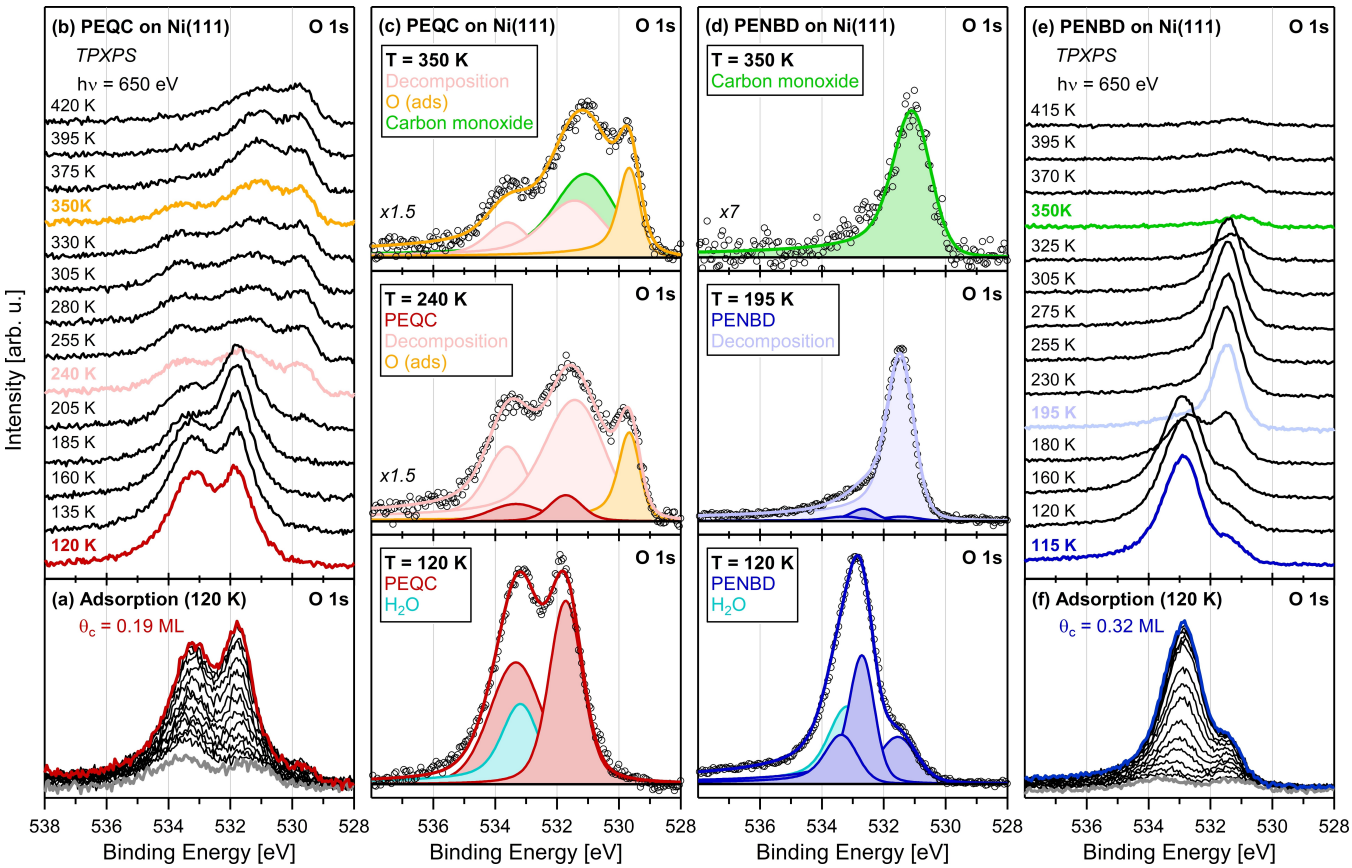

Figure 6. XP spectra of a) PEQC and f) PENBD in the O 1s region upon adsorption at low temperature on Ni(111). The thermal evolution during temperature-programmed XPS (TPXPS) experiments is depicted for selected spectra of b) PEQC and e) PENBD as waterfall plots; c), d) representative surface species are given with their corresponding color-coded fits, respectively.

© 2023 The Authors. Chemistry - A European Journal published by Wiley-VCH GmbH

15213765, 2023, 25, Downloaded from https://chemistry-europe.onlinelibrary.wiley.com/doi/10.1002/chem.202203759 by Freie Universitaet Berlin, Wiley Online Library on [24/05/2023]. See the Terms and Conditions (https://onlinelibrary.wiley.com/terms-and-conditions) on Wiley Online Library for rules of use; OA articles are governed by the applicable Creative Commons License

is in agreement with ester derivatives adsorbed on single crystal surfaces.[19,28,32]

For PENBD on Ni(111), the fit to the spectrum after adsorption at 120 K is shown in Figure 6d (blue). Again, the coadsorption of water was unavoidable during exposure yielding a peak at 533.1 eV (turquoise).[31] The spectrum is fitted with three additional peaks at 531.5, 532.7 and 533.3 eV (blue), with a fixed relative intensity ratio (1:2:1). The positions are shifted to lower binding energies by up to 600 meV in comparison to PEQC. Along to the results of Ontaneda et al.,[32] we attribute this to a stronger interaction of the oxygen atoms with the surface. Interestingly, on Pt(111) hardly any difference is observed in the O 1s spectra of PEQC and PENBD at 125 K (Figure S1). With only minor structural differences between PEQC and PENBD, remote to the oxygen atoms, different adsorption motifs of the molecules are expected. As PEQC features higher O 1s binding energies, the oxygen atoms of the ester group are likely to be not bound to the surface;[32] instead, stable adsorption by the QC framework and phenyl moiety is suggested. In contrast, for PENBD, we propose an "oxygen bound" geometry with the ester group pointing towards the surface. Our fits indicate two different binding fashions: The binding with two oxygen atoms to the surface leads to a very similar chemical environment for both atoms and is attributed to the peak at 532.7 eV; on the other hand, the two peaks at 531.5 and 533.3 eV, with identical fit area, are due to a binding and non-binding oxygen atom.[32] Notably, various rotational isomers of esters are known on Ni(111)[33] enabling different binding motifs. The pronounced desorption of PENBD on Ni(111) for relatively low temperatures of 270 K (Figure 5c) is attributed to the weaker Ni-oxygen interaction[34] compared to the Ni-carbon bond for PEQC. Our results thus indicate that the derivatization with extended ligands can determine the adsorption behavior of the molecule pair and hereby leads to very different desorption properties and decomposition pathways upon heating, which is addressed in the following.

The thermal evolution of PEQC on Ni(111) in the O 1s region is shown in Figure 6b as waterfall plot, along with selected fits in Figure 6c; the quantitative analysis is given in Figure 5b. Analogous to the PENBD experiment (see below), the water contributions desorb between 140 and 180 K, so that the intensity of the PEQC peaks increase slightly due to less damping. Starting at 180 K, a narrow peak appears at 529.6 eV, which is assigned to atomic oxygen on Ni(111) (orange).[25a,26,35] At the same time, two new peaks at 531.3 and 533.5 eV indicate the onset of the decomposition of PEQC (rose). This observation matches the conclusions derived from the C 1s experiment (see above). Heating to above 280 K gives rise to an additional peak at 531.0 eV (green), which is assigned to CO on a bridge site,[26] in line with the findings in the C 1s region.

The TPXPS experiment of PENBD on Ni(111) in the O 1s region is depicted in Figure 6e along with selected fits in Figure 6d, and the quantitative analysis in Figure 5d. Between 140 and 180 K, coadsorbed water desorbs, which is in agreement with findings in literature.[31b] Above 160 K, a new peak evolves at 531.4 eV (light blue). This clear shift of 1.3 eV of the main signal towards lower binding energy matches the spectral changes in the C 1s region at equivalent temperatures (see above). Therefore, a first reaction step is proposed which includes the oxygen atoms. Likely, this step is the detachment or fragmentation of the ester moiety.[25b] The decrease of about 25% of the oxygen coverage in comparison to the initial PENBD (note that for the carbon region an according increase is detected, see above) is attributed to different attenuation and diffraction conditions depending on the adsorption geometry of the newly formed species.[30] Starting at 280 K, a new peak emerges at 531.0 eV (Figure 6d, green), which fits to literature values of CO on Ni(111) in bridge position.[26] Simultaneously, the majority of the O 1s signal vanishes leaving only 16% of the previous surface coverage (Figure 5d), in very good agreement with the corresponding C 1s experiment (13% of total intensity remaining, see above).

Conclusion

We have investigated the surface chemistry of 2-carbethoxy-3-phenyl-norbornadiene/quadricyclane (PENBD/PEQC) on Pt(111) and Ni(111) by synchrotron radiation-based HR-XPS measurements. The adsorption of the two valence isomers and their thermal evolution was monitored in temperature-programmed experiments. For both surfaces, a spectroscopic distinction between the energy-rich PEQC and its energy-lean counterpart PENBD was possible upon exposure at temperatures between 115 and 125 K. On Pt(111), no "side-on" geometry is found for the molecule pair, as we observed no signs of the detachment of a hydrogen atom from the bridgehead methyl group. On Ni(111), the very distinct spectral appearance of PEQC and PENBD in the C 1s and O 1s regions indicates different adsorption motifs. Whereas PEQC is expected to bind by the QC framework and phenyl moiety, PENBD is adsorbed weaker in an "oxygen-bound" fashion, with the ester group likely oriented towards the surface.

Reaction pathways for both valence isomers on the two surfaces (Scheme 1) are proposed based on a quantitative evaluation of the corresponding TPXPS experiments. For Pt(111) as model catalyst surface, the onset of the cycloreversion reaction of PEQC to PENBD is found at 140 K, with the conversion complete at 230 K. Decomposition of PENBD occurs only at 300 K, when decomposition products assigned to CO and C–H fragments emerge on the surface. Notably, PENBD on Pt(111) is much more stable than unsubstituted NBD, which decomposes even at 190 K. The back reaction of PEQC to PENBD cannot be triggered thermally on Ni(111). Instead, individual decomposition routes begin at 160 and 180 K. Interestingly, for PENBD on Ni(111), about 90% of the surface species desorbs above 300 K; this is explained by the "oxygen-bound" adsorption geometry, which only allows for a weak surface interaction. Minor contributions from CO and C–H fragments remain on the surface. For PEQC, when heating higher than 180 K, atomic oxygen is observed next to these decomposition products.

Thus, we have demonstrated the dependence of the reactivity of derivatized NBD/QC species on the catalyst surface used. On Pt(111), the successfully monitored cycloreversion reaction of PEQC to PENBD fulfills the most important requirement of a MOST

© 2023 The Authors. Chemistry - A European Journal published by Wiley-VCH GmbH

15213765, 2023, 25, Downloaded from https://chemistry-europe.onlinelibrary.wiley.com/doi/10.1002/chem.202203759 by Freie Universitaet Berlin, Wiley Online Library on [24/05/2023]. See the Terms and Conditions (https://onlinelibrary.wiley.com/terms-and-conditions) on Wiley Online Library for rules of use; OA articles are governed by the applicable Creative Commons License

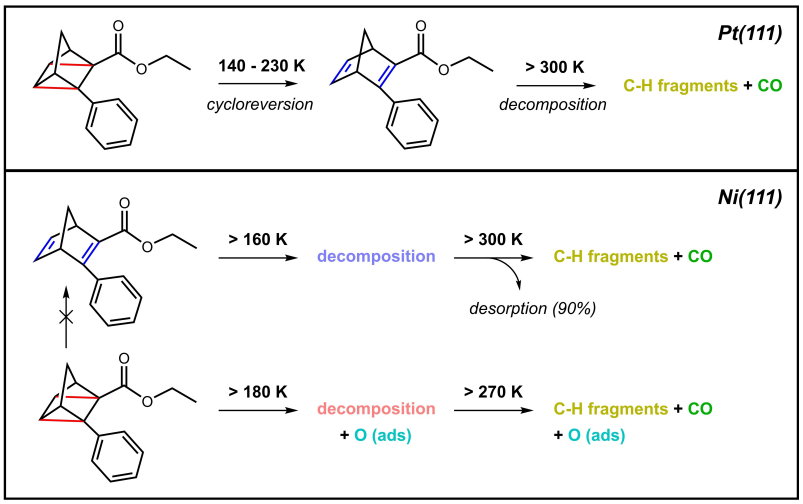

Scheme 1. Top: Proposed reaction pathway of PEQC on Pt(111). The cycloreversion reaction to PENBD occurs between 140 and 230 K with subsequent decomposition into C–H fragments and CO when the mixture is heated at > 300 K. Bottom: On Ni(111). There is no conversion of PEQC to PENBD, but individual decomposition steps begin at 160 and 180 K; there is pronounced desorption of PENBD above 300 K, and further fragmentation above 270 K for PEQC.

system; the experiments on Ni(111) provided insights into stability boundaries and desorption behavior of the derivatives, which is of interest for heterogeneously catalyzed processes to ensure a fully reversible energy storage cycle.

Experimental Section

X-ray photoelectron spectroscopy (XPS): All experiments were carried out in a transportable ultra-high-vacuum (UHV) apparatus; the setup is described in detail elsewhere.[36] The analysis chamber houses a hemispherical electron analyzer (Omicron EA 125U7 HR), and an evaporator for organic compounds. Surface cleaning and preparation is conducted in a separate preparation chamber, which includes, among other typical surface science tools, a sputter gun and LEED optics. The XPS measurements were performed using synchrotron radiation at BESSY II of Helmholtz-Zentrum Berlin, at beamlines UE56/2-PGM1 and -PGM2. The light incidence angle was 50°, and the spectra were acquired at normal emission. With an excitation energy of 380 eV for the C 1s and 650 eV for the O 1s region, total energy resolutions of 180 and 250 meV were achieved, respectively.

Prior to each adsorption experiment, the Pt(111) and Ni(111) single crystals were checked for cleanness by XPS. Ion bombardment (Ar^+, $E = 1.0$ keV, $I_S \sim 2$ μA) was used to remove impurities on the surfaces, with subsequent annealing to 1200 K. Residual carbon contaminations were removed by oxygen exposure at 800 K. 2-Carbethoxy-3-phenyl-norbornadiene/quadricyclane were purified by freeze–pump–thaw procedures. Deposition of both compounds onto the surface at ~120 K took place through their vapor pressure, with the exposure given in Langmuir ($1\ L = 10^{-6}$ Torr s). Coverages are denoted in ML (1 ML equals one adsorbed atom per surface atom), as determined by comparison to layers with well-defined coverage. These are the CO $c(4\times2)$ superstructure on Pt(111)[22,37] with a carbon coverage of 0.5 ML, and the closed graphene layer on Ni(111)[38] with a carbon coverage of 2 ML; the oxygen coverages are then calculated using the stoichiometric factor of 1/8 in the molecular structure. Temperature-programmed experiments[21,39] were performed with a heating rate of $\beta = 0.5\ K s^{-1}$ up to 550 K, using a bifilar coiled filament behind the crystal. To minimize beam damage, that is, X-ray induced reactions, we shifted the sample to a new position after every recorded spectrum. All XPS binding energies were referenced to the Fermi level, and a linear background was subtracted from the XP spectra. The quantitative analysis was performed by fitting the respective contributions in the XP spectra; the applied line shape is a convolution of Doniach-Šunjić[40] and Gaussian functions.

Molecule synthesis

2-Carbethoxy-3-phenyl-norbornadiene (PENBD): Ethyl-3-phenylpropiolate (5.55 g, 31.9 mmol, 1 equiv.) and cyclopentadiene (freshly cracked; 4.22 g, 63.8 mmol, 2 equiv.) were added to a pressure vial and the reaction was heated to 170 °C overnight, after degassing of the reaction mixture with argon for 5 min. Subsequently, the crude product was purified by fractionated vacuum distillation using a Vigreux column (bp = 123 °C at 4.6×10^{-2} mbar). PENBD was obtained as a colorless oil (4.59 g, 19.1 mmol, 60%). ^{1}H NMR (400 MHz, $CDCl_3$, 25 °C): $\delta = 7.54$–7.51 (m, 2H), 7.38–7.29 (m, 3H), 7.01–6.99 (m, 1H), 6.94–6.92 (m, 1H), 4.14 (qd, $J = 6.8$, 0.8 Hz, 2H), 4.08–4.06 (m, 1H), 3.87–3.85 (m, 1H), 2.26 (dt, $J = 6.4$, 1.6 Hz, 1H), 2.06 (dt, $J = 6.8$, 1.6 Hz, 1H), 1.22 (t, $J = 7.1$ Hz, 3H) ppm; see Figure S4.

2-Carbethoxy-3-phenyl-quadricyclane (PEQC): PENBD (300 mg, 1.25 mmol) was dissolved in deuterated chloroform and irradiated with an UV-LED (Seoul Viosys, CUD1AF4D, 310 nm, 30 mW) overnight. Afterwards, the solvent was removed, and the crude product was purified by flash chromatography (hexane/EtOAc 9.5:0.5, *v/v*). PEQC was obtained as a white solid (294 mg, 1.23 mmol, 98%). ^{1}H NMR (400 MHz, $CDCl_3$, 25 °C): $\delta = 7.29$–7.23 (m, 4H), 7.20–7.14 (m, 1H), 3.97 (qd, $J = 7.2$, 0.4 Hz, 2H), 2.56–2.53 (m, 1H), 2.45–2.42 (m, 1H), 2.36 (dt, $J = 11.6$, 1.4 Hz, 1H), 2.23–2.21 (m, 1H), 2.12 (dt, $J = 11.6$, 1.4 Hz, 1H), 1.72–1.69 (m, 1H), 1.03 (t, $J = 7.2$ Hz, 3H) ppm; see Figure S5.

Acknowledgements

Support for this work was granted by the Deutsche Forschungsgesellschaft (DFG) – Project no. 392607742 and the Cluster of Excellence "Engineering of Advanced Materials". We thank

© 2023 The Authors. Chemistry - A European Journal published by Wiley-VCH GmbH

15213765, 2023, 25, Downloaded from https://chemistry-europe.onlinelibrary.wiley.com/doi/10.1002/chem.202203759 by Freie Universitaet Berlin, Wiley Online Library on [24/05/2023]. See the Terms and Conditions (https://onlinelibrary.wiley.com/terms-and-conditions) on Wiley Online Library for rules of use; OA articles are governed by the applicable Creative Commons License

Helmholtz-Zentrum Berlin for the allocation of synchrotron radiation beamtime and the BESSY II staff for support during beamtime. Open Access funding enabled and organized by Projekt DEAL.

Conflict of Interest

The authors declare no conflict of interest.

Data Availability Statement

The data that support the findings of this study are available from the corresponding author upon reasonable request.

Keywords: catalysis · energy storage · MOST system · photoelectron spectroscopy · surface reactions

[1] AGEB AG Energiebilanzen e.V., *Energy Consumption in Germany in 2021*, https://ag-energiebilanzen.de/wp-content/uploads/2022/06/AGEB_Jahresbericht2020_20220613_engl_Web.pdf (retrieved 22.11.2022).
[2] D. Jahn, S. Korolczuk, *Environ. Politics* **2012**, *21*, 159–164.
[3] a) A. Lennartson, A. Roffey, K. Moth-Poulsen, *Tetrahedron Lett.* **2015**, *56*, 1457–1465; b) C. L. Sun, C. Wang, R. Boulatov, *ChemPhotoChem* **2019**, *3*, 268–283; c) Z. Wang, A. Roffey, R. Losantos, A. Lennartson, M. Jevric, A. U. Petersen, M. Quant, A. Dreos, X. Wen, D. Sampedro, K. Börjesson, K. Moth-Poulsen, *Energy Environ. Sci.* **2019**, *12*, 187–193; d) Z. Wang, P. Erhart, T. Li, Z.-Y. Zhang, D. Sampedro, Z. Hu, H. A. Wegner, O. Brummel, J. Libuda, M. B. Nielsen, K. Moth-Poulsen, *Joule* **2021**, *5*, 3116–3136; e) K. Börjesson, A. Lennartson, K. Moth-Poulsen, *ACS Sustainable Chem. Eng.* **2013**, *1*, 585–590; f) T. J. Kucharski, Y. C. Tian, S. Akbulatov, R. Boulatov, *Energy Environ. Sci.* **2011**, *4*, 4449–4472; g) K. Moth-Poulsen, D. Ćoso, K. Börjesson, N. Vinokurov, S. K. Meier, A. Majumdar, K. P. C. Vollhardt, R. A. Segalman, *Energy Environ. Sci.* **2012**, *5*, 8534; h) Q. Qiu, Y. Shi, G. G. D. Han, *J. Mater. Chem. C* **2021**, *9*, 11444–11463.
[4] a) H. Taoda, K. Hayakawa, K. Kawase, H. Yamakita, *J. Chem. Eng. Jpn.* **1987**, *20*, 265–270; b) Z. Wang, R. Losantos, D. Sampedro, M. Morikawa, K. Börjesson, N. Kimizuka, K. Moth-Poulsen, *J. Mater. Chem. A* **2019**, *7*, 15042–15047; c) H. M. Bandara, S. C. Burdette, *Chem. Soc. Rev.* **2012**, *41*, 1809–1825.
[5] a) D. Schulte-Frohlinde, H. Blume, H. Güsten, *J. Phys. Chem.* **1962**, *66*, 2486–2491; b) C. Bastianelli, V. Caia, G. Cum, R. Gallo, V. Mancini, *J. Chem. Soc. Perkin Trans. 2* **1991**, 679–683.
[6] a) K. Börjesson, D. Ćoso, V. Gray, J. C. Grossman, J. Guan, C. B. Harris, N. Hertkorn, Z. Hou, Y. Kanai, D. Lee, J. P. Lomont, A. Majumdar, S. K. Meier, K. Moth-Poulsen, R. L. Myrabo, S. C. Nguyen, R. A. Segalman, V. Srinivasan, W. B. Tolman, N. Vinokurov, K. P. Vollhardt, T. W. Weidman, *Chem. Eur. J.* **2014**, *20*, 15587–15604; b) Y. Kanai, V. Srinivasan, S. K. Meier, K. P. Vollhardt, J. C. Grossman, *Angew. Chem. Int. Ed.* **2010**, *49*, 8926–8929; *Angew. Chem.* **2010**, *122*, 9110–9113.
[7] G. S. Hammond, N. J. Turro, A. Fischer, *J. Am. Chem. Soc.* **1961**, *83*, 4674–4675.
[8] H. Taoda, K. Hayakawa, K. Kawase, *J. Chem. Eng. Jpn.* **1987**, *20*, 335–338.
[9] H. Hogeveen, H. C. Volger, *J. Am. Chem. Soc.* **1967**, *89*, 2486–2487.
[10] X. W. An, Y. D. Xie, *Thermochim. Acta* **1993**, *220*, 17–25.
[11] M. Quant, A. Lennartson, A. Dreos, M. Kuisma, P. Erhart, K. Börjesson, K. Moth-Poulsen, *Chem. Eur. J.* **2016**, *22*, 13265–13274.
[12] a) A. D. Dubonosov, V. A. Bren, V. A. Chernoivanov, *Russ. Chem. Rev.* **2002**, *71*, 917–927; b) V. Gray, A. Lennartson, P. Ratanalert, K. Börjesson, K. Moth-Poulsen, *Chem. Commun.* **2014**, *50*, 5330–5332; c) M. Mansø, B. E. Tebikachew, K. Moth-Poulsen, M. B. Nielsen, *Org. Biomol. Chem.* **2018**, *16*, 5585–5590.
[13] a) K. Jorner, A. Dreos, R. Emanuelsson, O. El Bakouri, I. Fdez. Galván, K. Börjesson, F. Feixas, R. Lindh, B. Zietz, K. Moth-Poulsen, H. Ottosson, *J. Mater. Chem. A* **2017**, *5*, 12369–12378; b) M. Jevric, A. U. Petersen, M. Mansø, S. Kumar Singh, Z. Wang, A. Dreos, C. Sumby, M. B. Nielsen, K. Börjesson, P. Erhart, K. Moth-Poulsen, *Chem. Eur. J.* **2018**, *24*, 12767–12772; c) A. Dreos, Z. Wang, J. Udmark, A. Ström, P. Erhart, K. Börjesson, M. B. Nielsen, K. Moth-Poulsen, *Adv. Energy Mater.* **2018**, *8*, 1703401; d) M. Mansø, A. U. Petersen, Z. Wang, P. Erhart, M. B. Nielsen, K. Moth-Poulsen, *Nat. Commun.* **2018**, *9*, 1945; e) M. Manso, L. Fernandez, Z. Wang, K. Moth-Poulsen, M. B. Nielsen, *Molecules* **2020**, *25*, 322; f) J. Orrego-Hernández, A. Dreos, K. Moth-Poulsen, *Acc. Chem. Res.* **2020**, *53*, 1478–1487; g) A. Kunz, H. A. Wegner, *ChemSystemsChem* **2020**, *3*, e2000035.
[14] U. Bauer, S. Mohr, T. Dopper, P. Bachmann, F. Späth, F. Düll, M. Schwarz, O. Brummel, L. Fromm, U. Pinkert, A. Görling, A. Hirsch, J. Bachmann, H.-P. Steinrück, J. Libuda, C. Papp, *Chem. Eur. J.* **2017**, *23*, 1613–1622.
[15] U. Bauer, L. Fromm, C. Weiß, P. Bachmann, F. Späth, F. Düll, J. Steinhauer, W. Hieringer, A. Görling, A. Hirsch, H.-P. Steinrück, C. Papp, *J. Phys. Chem. C* **2018**, *123*, 7654–7664.
[16] U. Bauer, L. Fromm, C. Weiß, F. Späth, P. Bachmann, F. Düll, J. Steinhauer, S. Matysik, A. Pominov, A. Görling, A. Hirsch, H.-P. Steinrück, C. Papp, *J. Chem. Phys.* **2019**, *150*, 184706.
[17] F. Hemauer, U. Bauer, L. Fromm, C. Weiß, A. Leng, P. Bachmann, F. Düll, J. Steinhauer, V. Schwaab, R. Grzonka, A. Hirsch, A. Görling, H. P. Steinrück, C. Papp, *ChemPhysChem* **2022**, *23*, e202200199.
[18] a) P. Lorenz, T. Luchs, A. Hirsch, *Chem. Eur. J.* **2021**, *27*, 4993–5002; b) W. Alex, P. Lorenz, C. Henkel, T. Clark, A. Hirsch, D. M. Guldi, *J. Am. Chem. Soc.* **2022**, *144*, 153–162.
[19] F. Bournel, C. Laffon, P. Parent, G. Tourillon, *Surf. Sci.* **1996**, *350*, 60–78.
[20] R. Zhang, A. J. Hensley, J. S. McEwen, S. Wickert, E. Darlatt, K. Fischer, M. Schoppke, R. Denecke, R. Streber, M. Lorenz, C. Papp, H. P. Steinrück, *Phys. Chem. Chem. Phys.* **2013**, *15*, 20662–20671.
[21] C. Papp, H.-P. Steinrück, *Surf. Sci. Rep.* **2013**, *68*, 446–487.
[22] M. Kinne, T. Fuhrmann, C. M. Whelan, J. F. Zhu, J. Pantförder, M. Probst, G. Held, R. Denecke, H. P. Steinrück, *J. Chem. Phys.* **2002**, *117*, 10852–10859.
[23] C. Papp, T. Fuhrmann, B. Tränkenschuh, R. Denecke, H. P. Steinrück, *Phys. Rev. B* **2006**, *73*, 235426.
[24] A. Wiltner, C. Linsmeier, *Phys. Status Solidi* **2004**, *201*, 881–887.
[25] a) M. Castonguay, J. R. Roy, P. H. McBreen, *Langmuir* **2000**, *16*, 8306–8310; b) E. Zahidi, M. Castonguay, P. McBreen, *J. Am. Chem. Soc.* **1994**, *116*, 5847–5856.
[26] G. Held, J. Schuler, W. Sklarek, H. P. Steinrück, *Surf. Sci.* **1998**, *398*, 154–171.
[27] a) S. Lehwald, H. Ibach, *Surf. Sci.* **1979**, *89*, 425–445; b) C. Papp, R. Denecke, H.-P. Steinrück, *Langmuir* **2007**, *23*, 5541–5547.
[28] M. Castonguay, J. R. Roy, A. Rochefort, P. H. McBreen, *J. Am. Chem. Soc.* **2000**, *122*, 518–524.
[29] H. P. Steinrück, T. Fuhrmann, C. Papp, B. Tränkenschuh, R. Denecke, *J. Chem. Phys.* **2006**, *125*, 204706.
[30] a) C. J. Powell, A. Jablonski, *Nucl. Instrum. Methods Phys. Res. Sect. A* **2009**, *601*, 54–65; b) D. P. Woodruff, A. M. Bradshaw, *Rep. Prog. Phys.* **1994**, *57*, 1029–1080.
[31] a) W. Kuch, M. Schulze, W. Schnurnberger, K. Bolwin, *Surf. Sci.* **1993**, *287–288*, 600–604; b) T. Pache, H. P. Steinrück, W. Huber, D. Menzel, *Surf. Sci.* **1989**, *224*, 195–214.
[32] J. Ontaneda, R. E. J. Nicklin, A. Cornish, A. Roldan, R. Grau-Crespo, G. Held, *J. Phys. Chem. C* **2016**, *120*, 27490–27499.
[33] a) E. Zahidi, M. Castonguay, P. H. McBreen, *J. Phys. Chem.* **1995**, *99*, 17906–17916; b) J. Wang, M. Castonguay, J. R. Roy, E. Zahidi, P. H. McBreen, *J. Phys. Chem. B* **1999**, *103*, 4382–4386.
[34] Y. Bai, D. Kirvassilis, L. Xu, M. Mavrikakis, *Surf. Sci.* **2019**, *679*, 240–253.
[35] M. K. Rajumon, K. Prabhakaran, C. N. R. Rao, *Surf. Sci.* **1990**, *233*, L237-L242.
[36] R. Denecke, M. Kinne, C. M. Whelan, H.-P. Steinrück, *Surf. Rev. Lett.* **2002**, *09*, 797–801.
[37] F. Bondino, G. Comelli, F. Esch, A. Locatelli, A. Baraldi, S. Lizzit, G. Paolucci, R. Rosei, *Surf. Sci.* **2000**, *459*, L467-L474.
[38] a) W. Zhao, S. M. Kozlov, O. Höfert, K. Gotterbarm, M. P. A. Lorenz, F. Viñes, C. Papp, A. Görling, H.-P. Steinrück, *J. Phys. Chem. Lett.* **2011**, *2*, 759–764; b) R. Addou, A. Dahal, P. Sutter, M. Batzill, *Appl. Phys. Lett.* **2012**, *100*, 021601.
[39] A. Baraldi, G. Comelli, S. Lizzit, D. Cocco, G. Paolucci, R. Rosei, *Surf. Sci.* **1996**, *367*, L67-L72.
[40] S. Doniach, M. Sunjic, *J. Phys. C Solid State Phys.* **1970**, *3*, 285–291.

Manuscript received: December 1, 2022
Accepted manuscript online: February 25, 2023
Version of record online: March 23, 2023

© 2023 The Authors. Chemistry - A European Journal published by Wiley-VCH GmbH

15213765, 2023, 25, Downloaded from https://chemistry-europe.onlinelibrary.wiley.com/doi/10.1002/chem.202203759 by Freie Universitaet Berlin, Wiley Online Library on [24/05/2023]. See the Terms and Conditions (https://onlinelibrary.wiley.com/terms-and-conditions) on Wiley Online Library for rules of use; OA articles are governed by the applicable Creative Commons License